

Pomeron interaction in the perturbative QCD

J.Bartels¹ and M.A.Braun²

¹Hamburg University, Germany,

²S.Petersburg State University, Russia

Abstract. Formation of the triple pomeron vertices in processes $P \rightarrow PP \rightarrow PPP$ and $PP \rightarrow P \rightarrow PP$ is studied in the BFKL-Bartels approach. It is demonstrated that successive splittings of the pomeron indeed generate the standard triple pomeron vertex in agreement with the dipole approach. In contrast, in the process $PP \rightarrow P \rightarrow PP$ the improper part of the vertex is found missing. Significance of this result is discussed in the framework of the theory of interacting pomerons.

1 Motivation

In the perturbative QCD strong interactions are mediated by exchange of QCD pomerons ("BFKL pomerons", P), which are bound states of pairs of reggeized gluons ("reggeons") [1]. The latter are extension of the standard gluons to complex angular momenta. Pomerons can interact either by splitting of a pomeron in two ($P \rightarrow PP$) or by fusing of a pair of pomerons into one ($PP \rightarrow P$). For the splitting the corresponding triple pomeron vertex was constructed both in the BFKL approach [2, 3] and dipole picture [4]. It is illustrated in Fig. 1, in which the pomerons coupled to the projectile and targets are shown as ladders of interacting reggeons. In the transverse coordinate space the three participating

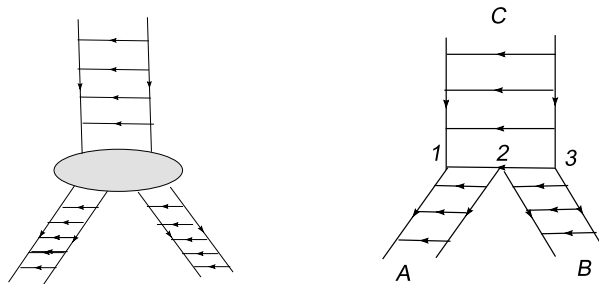


Figure 1. The triple pomeron vertex

pomerons are connected as shown in the right part of Fig. 1. The connecting line passing through

points r_1, r_2 and r_3 corresponds to factor [5]

$$\Gamma(r_1, r_2, r_3) = -\frac{g^4 N_c r_{13}^2 \nabla_1^2 \nabla_3^2}{4\pi^3 r_{12}^2 r_{23}^2}, \quad (1)$$

where $r_{12} = r_1 - r_2$ and so on.

The triple pomeron vertex has played an important role in applications of both the BFKL and dipole approaches to observables. It lies at the origin of the structure function of the heavy nucleus, as given by the Balitski-Kovchegov equation [6, 7], which sums pomeron fan diagrams with this vertex (Fig. 2, left). It is also responsible for the pomeron self-mass (Fig. 2, center), which was calculated

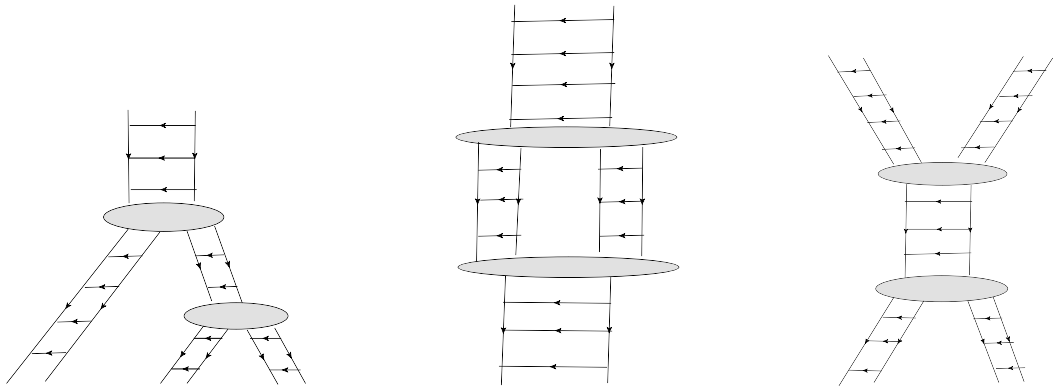


Figure 2. Pomeron fans, self-mass, and transition $PP \rightarrow P \rightarrow PP$

in [8–11].

The splitting and fusing of pomerons by vertex Γ was formalized in the effective pomeron action introduced in [12] in which pomerons are described as bilocal fields $\phi(r_1, r_2)$ with the interaction Lagrangian

$$L_I = \frac{2\alpha_s^2 N_c}{\pi} \int \frac{d^2 r_1 d^2 r_2 d^2 r_3}{r_{12}^2 r_{23}^2 r_{31}^2} \phi(r_1, r_2) \phi(r_2, r_3) r_{13}^4 \nabla_1^2 \nabla_3^2 \phi^\dagger(r_1, r_3) + h.c. \dots \quad (2)$$

As follows from this action in the second order, apart from the self-mass contribution of Fig.2,center, transition $PP \rightarrow P \rightarrow PP$, Fig. 2,right, takes place.

However in the BFKL approach the triple pomeron vertex was derived only for the case of a single splitting of a pomeron in two. Neither two nor more consecutive splittings corresponding to Fig. 2. left and right, have been studied and it was not demonstrated that these processes are governed by two and more vertices Γ . For fan diagrams Fig. 2, left, there exists an alternative derivation in the dipole picture, which, translated into the BFKL language, indicated that indeed in consecutive splittings exactly vertices Γ appear [13, 14]. However in view of the rather indirect correspondence between the dipole and BFKL approaches it would be desirable to derive this result within the latter approach.

More complicated is the situation with the transition $PP \rightarrow P \rightarrow PP$. In this case the dipole approach cannot be used and the derivation of Fig. 2, right, is a problem.

The point is that within the BFKL approach Γ is obtained after summation of transitions of two, three and four reggeons from the colourless short range projectile ($q\bar{q}$ loop) to the two final pomerons.

Suppressing evolution in rapidity, which does not influence the triple pomeron vertex, the latter is obtained from the sum of diagrams shown in Fig. 3.

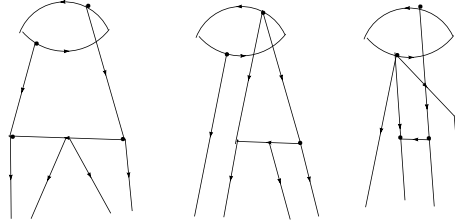


Figure 3. The triple pomeron vertex. Points refer to the coordinate space

Of the three diagrams which sum into Γ , transitions $P \rightarrow PP \rightarrow PPP$ (Fig. 2, left) and $PP \rightarrow P \rightarrow PP$ (Fig. 2, right) contain only the first.

We demonstrate, in the first place, that additional diagrams for $P \rightarrow PP \rightarrow PPP$ provide the necessary contributions which transform the kernel $K_{2 \rightarrow 4}$ for the second splitting into Γ in accordance with the results obtained in the dipole approach. On the other hand, in the transition $PP \rightarrow P \rightarrow PP$ additional diagrams with three and four intermediate reggeons seem to give only a part of the contributions to convert one of the simple kernels $K_{2 \rightarrow 4}$ into Γ . The rest of the necessary contributions remains missing. In case no new contributions are found, in the transition $PP \rightarrow P \rightarrow PP$ the triple pomeron vertex degenerates into the splitting kernel $K_{2 \rightarrow 4}$, which is in fact one half of the proper part of the standard Γ .

2 Three-pomeron vertex in the reggeon approach

The basis of the derivation of the three-pomeron vertex in the reggeon approach is the so-called bootstrap property of reggeon interaction. It consists in fusing of three and four reggeons in the adjoint colour representation into a single reggeon when they are coupled in a special manner to the colourless projectile. This special coupling is provided by a $q\bar{q}$ loop. In this case the amplitudes for coupling of three and four reggeons to the loop, D_{30} and D_{40} are expressed via amplitude D_{20} with only two reggeons coupled to the loop:

$$D_{30}^{a_1 a_2 a_3}(1, 2, 3) = -\frac{1}{2} f^{a_1 a_2 a_3} g (D_{20}(2, 31) - D_{20}(1, 23) - D_{20}(3, 12)), \tag{3}$$

$$D_{40}^{a_1 a_2 a_3 a_4}(1, 2, 3, 4) = -d^{a_1 a_2 a_3 a_4} D_{40}^{1234}(1, 2, 3, 4) - d^{a_2 a_1 a_3 a_4} D_{40}^{2134}(1, 2, 3, 4), \tag{4}$$

where

$$D_{40}^{1234} = g^2 (D_{20}(1, 234) + D_{20}(123, 4) - D_{20}(14, 23)), \tag{5}$$

$$D_{40}^{2134} = g^2 (D_{20}(2, 134) + D_{20}(124, 3) - D_{20}(12, 34) - D_{20}(13, 24)) \tag{6}$$

for two states of 4 reggeons, which differ in their order on the surface of a cylinder (indicated by the upper index). Here 12 means $q_1 + q_2$, a_i are colour indices and $d^{a_1 a_2 a_3 a_4} = \text{Tr}(t_1^a t_2^a t_3^a t_4^a + t_4^a t_3^a t_2^a t_1^a)$. The bootstrap ensures that evolution does not change these relations, that is the full amplitudes D_3 and D_4 for transition from the loop to 3 and 4 reggeons with all BFKL interactions and transitions from 2 to 3 and from 2 to 4 reggeons is given by the same formulas Eqs. (3), (5) and (6) with D_{20} substituted

by the BFKL pomeron D_2 ('reggeization') As a result transitions to 2 final pomerons all turn out to start also from the pomeron state and so can be expressed via the triple pomeron vertex. In fact the equation for this amplitude has a structure of a Shroedinger equation in rapidity and transverse momenta with certain inhomogeneous terms, which apart from the direct interaction with the $q\bar{q}$ loop, represent transitions into the two-pomeron state from two, three and four evolved reggeons coming from the loop. The three-pomeron vertex can be found from these latter inhomogeneous terms

$$D_{2\rightarrow 2P}^{(0)} + D_{3\rightarrow 2P}^{(0)} + D_{4\rightarrow 2P}^{(0)} = \Gamma D_{20} + R_{2P}^{(6)}, \tag{7}$$

where $R_{2P}^{(6)}$ is the reggeized D_{40} in order g^6 .

It is essential that this result does not use the explicit form of function $D_{20}(1, 2)$ and is valid if one substitutes D_{20} with arbitrary function $F_2(1, 2)$ which vanishes when q_1 or q_2 vanishes. It is only important that the impact factors F_3 and F_4 for 3 and 4 reggeons are related to F_2 in the same way as D_{30} and D_{40} to D_{20} .

3 Pomeron fan diagrams

In the fan diagrams (Fig. 2, left) in the first splitting all contributions from Fig. 3 take part, so that the standard vertex Γ is formed. However already in the second splitting there seems to enter only the first contribution. However in fact one finds two additional diagrams in which instead of the first splitting into 4 reggeons there appear splittings into 5 and 6 reggeons, shown in Fig. 4.

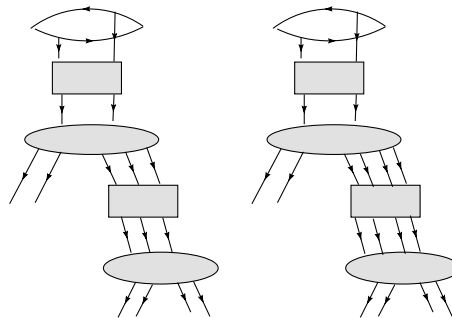


Figure 4. Additional pomeron fan diagrams to be added to Fig.2, left

As we shall demonstrate they convert vertex $K_{2\rightarrow 3}$ to the standard vertex Γ .

4 reggeons after the first splitting

After the first splitting we have the general 4-reggeon amplitude D_4 . Its part corresponding to the final state of two pomeron states made of reggeons 1,2 and 3,4 is given by $D_4^{a_1 a_2 a_3 a_4} = \delta_{a_1 a_2} \delta_{a_3 a_4} D_4(1, 2, 3, 4)$. Amplitude $D_4(1, 2, 3, 4)$ can be expressed via function

$$G(1, 2, 3) = K_{3\leftarrow 2}(1, 2, 3)D_2 + D_2(1, 23)(\omega(2) - \omega(23)) + D_2(12, 3)(\omega(2) - \omega(12)), \tag{8}$$

where $K_{2\rightarrow 3}$ describes transition from 2 to 3 reggeons and ω is the reggeon trajectory.

$$D_4(1, 2, 3, 4) = \frac{1}{2}g^2 \{G(1, 23, 4) + G(2, 13, 4) + G(1, 24, 3) + G(2, 14, 3)\}.$$

Coupling to the pomeron $P(1, 2)$ we obtain $g^2(G(1, 23, 4) + G(1, 24, 3)) \otimes P(1, 2)$. Here \otimes means integration over the pair of intermediate momenta. Introducing function $f(3, 4) = G(1, 23, 4) \otimes g^2 P(1, 2)$ we find that before the second splitting the final 4-gluon amplitude is coupled to a symmetric function $F_2(3, 4) = f(3, 4) + f(4, 3)$. It takes the role of the loop D_{20} for the second splitting.

5 reggeons after the first splitting

Here before the second splitting we find amplitude D_5 [17] for transition of the initial pomeron into five outgoing reggeons, two of which 1 and 2 are to transform into the outgoing pomeron and the remaining three, 3, 4 and 5, serve as ingoing for the second splitting. D_5 contains 10 terms, all are expressed via D_4 . Only three terms contribute to our colour structure. The first of them can be written in terms of function G as follows

$$(1) = \delta_{a_1 a_2} f^{a_3 a_4 a_5} \frac{1}{2} g^2 N_c^2 \{G(1, 234, 5) + G(2, 134, 5) + G(1, 25, 34) + G(2, 15, 34)\}. \quad (9)$$

Coupling 1 and 2 to the outgoing pomeron we get $(1) \otimes P(1, 2) = f^{a_3 a_4 a_5} F(34, 5)$, where F was defined above.

The remaining two terms give results corresponding to interchanges $(4 \leftrightarrow 5)$ and $(3 \leftrightarrow 4)$ and in this way will add terms corresponding to the full interaction with the $q\bar{q}$ loop: $(2) \otimes P(1, 2) = -f^{a_3 a_4 a_5} (F(35, 4))$ and $(3) \otimes P(1, 2) = f^{a_3 a_4 a_5} F(45, 3)$.

In the sum we get the impact factor for transition to 3 reggeons 3, 4 and 5

$$F_3 = \frac{1}{2} g f^{a_3 a_4 a_5} ((1) + (2) + (3)) = \frac{1}{2} g f^{a_3 a_4 a_5} (F(34, 5) + F(45, 3) - F(35, 4)) \quad (10)$$

exactly following the form (3).

6 gluons after the first splitting

The corresponding amplitude D_6 satisfies the Schroedinger equation with 6 inhomogeneous terms [17]. Only two of them give a non-zero contribution in our colour configuration: $T_1 = \sum d^{a_1 a_2 a_3 a_4} \delta_{a_5 a_6} I(1, 2, 3, 4|5, 6)$ and $T_2 = \sum d^{a_2 a_1 a_3 a_4} \delta_{a_5 a_6} J(1, 2, 3, 4|5, 6)$. The sums go over all partitions of reggeons into two groups with 4 reggeons in one of them and 2 in the other.

We start with T_1 . The relevant term from it is $T_1 = \delta_{a_1 a_2} d^{a_3 a_4 a_5 a_6} I(3, 4, 5, 6, 1, 2)$. Here according to [17]

$$I(3, 4, 5, 6|1, 2) = -g^2 (D_4(3, 456, 1, 2) + D_4(345, 6, 1, 2) - D_4(36, 45, 1, 2)). \quad (11)$$

Via function G .

$$D_4(3, 456, 1, 2) = \frac{1}{2} g^2 [G(3, 456, 2) + G(456, 13, 2) + G(3, 456, 1) + G(456, 32, 1)], \quad (12)$$

$$D_4(345, 6, 1, 2) = \frac{1}{2} g^2 [G(345, 16, 2) + G(6, 345, 2) + G(345, 26, 1) + G(6, 345, 1)], \quad (13)$$

$$D_4(36, 45, 1, 2) = \frac{1}{2} g^2 [G(36, 451, 2) + G(45, 361, 2) + G(36, 452, 1) + G(45, 362, 1)]. \quad (14)$$

Convolution with the pomeron $P(1, 2)$ gives

$$T_3 \otimes P(1, 2) = -g^2 d^{a_3 a_4 a_5 a_6} (F_2(456, 3) + F_2(6, 345) - F_2(36, 45)). \quad (15)$$

Comparing with (5) we observe that it is the correct structure for D_{40} . for the order of gluons 1234.

Now T_2 . The relevant term from it is $T_2 = \delta_{a_1 a_2} d^{a_4 a_3 a_5 a_6} J(4, 3, 5, 6, 1, 2)$ where from [17]

$$J(4, 3, 5, 6|2,) = -g^2 (D_4(456, 3, 2, 1) + D_4(346, 5, 2, 1) - D_4(34, 56, 2, 1) - D_4(45, 36, 2, 1)). \quad (16)$$

In terms of G

$$D_4(456, 3, 2, 1) = \frac{1}{2}g^2 [G(456, 32, 1) + G(42, 356, 1) + G(456, 31, 2) + G(41, 356, 2)],$$

$$D_4(346, 5, 2, 1) = \frac{1}{2}g^2 [G(346, 52, 1) + G(52, 346, 1) + G(346, 51, 2) + G(51, 346, 2)],$$

$$D_4(34, 56, 2, 1) = \frac{1}{2}g^2 [G(34, 562, 1) + G(56, 342, 1) + G(34, 561, 2) + G(56, 341, 2)],$$

$$D_4(45, 36, 2, 1) = \frac{1}{2}g^2 [G(45, 362, 1) + G(36, 452, 1) + G(45, 361, 2) + G(36, 451, 2)].$$

Convoluting with pomeron $P(1, 2)$ we find

$$T_4 \otimes P(1, 2) = -g^2 d^{a_4 a_3 a_5 a_6} [F_2(4, 356) + F_2(5, 345) - F_2(35, 46) - F_2(34, 56)]. \quad (17)$$

This has the same structure as the term D_{40} for the order or reggeons 2134., Eq. (6).

So collecting our results we see that the initial states for the second evolution into 4 reggeons 3456 are exactly the same as for the evolution into 4 reggeons in Fig. 3 with the only difference that loops D_{20} are substituted by functions F_2 . As a result due to Eq. (7) the second splitting in Fig. 2, left, will be accomplished by the same vertex Γ as the first splitting, in accordance with the results from the dipole picture.

4 Transitions $PP \rightarrow P \rightarrow PP$

In this section we discuss the possibility to obtain the structure shown in Fig. 2, right, in which two initial pomerons go into the intermediate pomeron and then into two final pomerons via the vertex Γ . As stressed in the introduction, vertex Γ is local in rapidity, has a fixed order g^8 and does not depend on y . So, to locate it in diagrams, we can neglect evolution in rapidity and study diagrams of order g^8 apart from the g -dependence of impact factors. This means that our aim reduces to study if we can find diagrams of order g^8 which, added to the contribution of the diagram in Fig. 5,A, transform it into the diagram in Fig. 5,B.

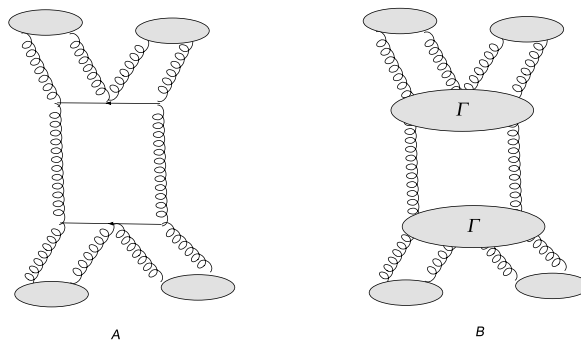


Figure 5. $PP \rightarrow P \rightarrow PP$ with two $K_{2 \rightarrow 4}$ (A) and with two Γ (B) in the lowest order

All typical diagrams in this order are illustrated in Fig. 6. Apart from the trivial term with two

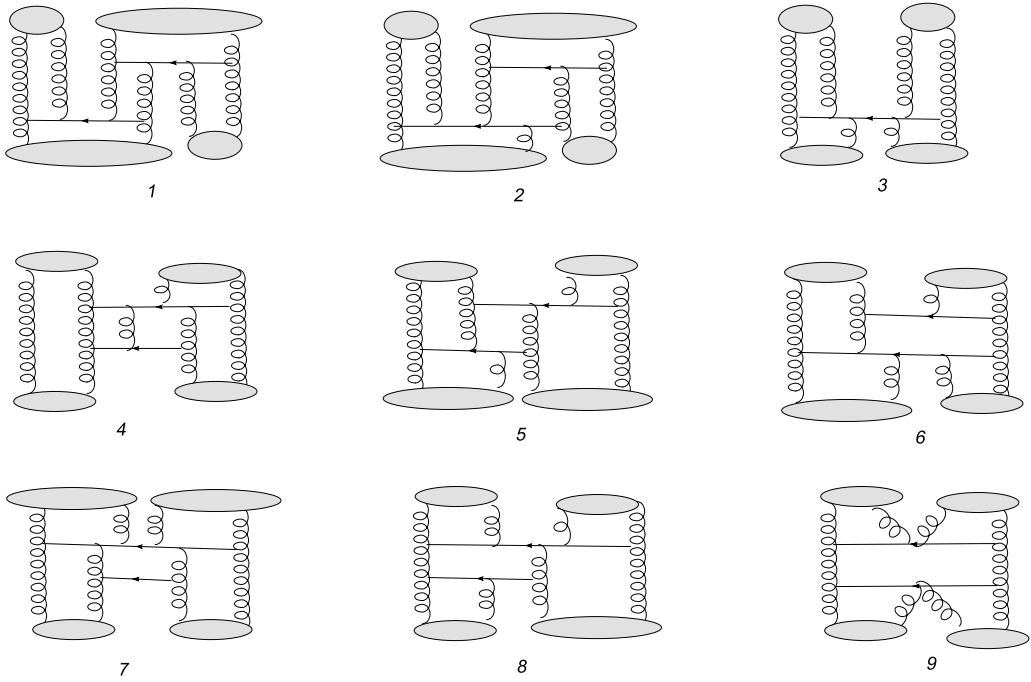


Figure 6. Diagrams of order g^8

kernels $K_{2 \rightarrow 4}$ possible candidates for the necessary additional contributions are reduced to diagrams 7, 8 and similar ones with the targets and projectile exchanged (3 and 6). Note that after convolution with, say, the initial pomerons these terms are to depend on only one variable.

Diagram in Fig.6,8

The diagram in Fig. 6,8 contains the kernel $K_{3 \rightarrow 4}$ [18]. It is composed of three parts shown graphically in Fig. 7. . After convolution of $K_{3 \rightarrow 4}$ with the upper impact factors we find one term in

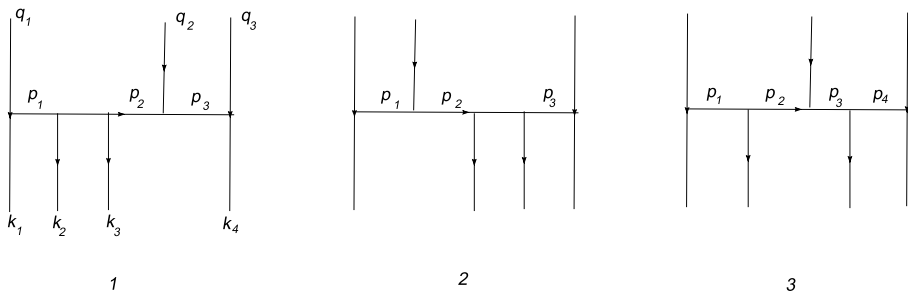


Figure 7. Kernel $K_{3 \rightarrow 4}$

part 1 and another one in part 2 which give the necessary structure $g(F_2(q_1, q_{23}) + F_2(q_3, q_{12}))/2$. So contributions from 3 intermediate reggeons give two of the necessary contributions to F_3 but the third term $-gF_2(q_2, q_{13})/2$ is missing.

Diagram in Fig.6,7

The diagram in Fig. 6,7 contains kernel $K_{4 \rightarrow 4}$ It is composed of six parts shown graphically in Fig. 8. . Four of them 1,2,3 and 6 can be expressed via the already known 3 parts of $K_{3 \rightarrow 4}$. parts 4

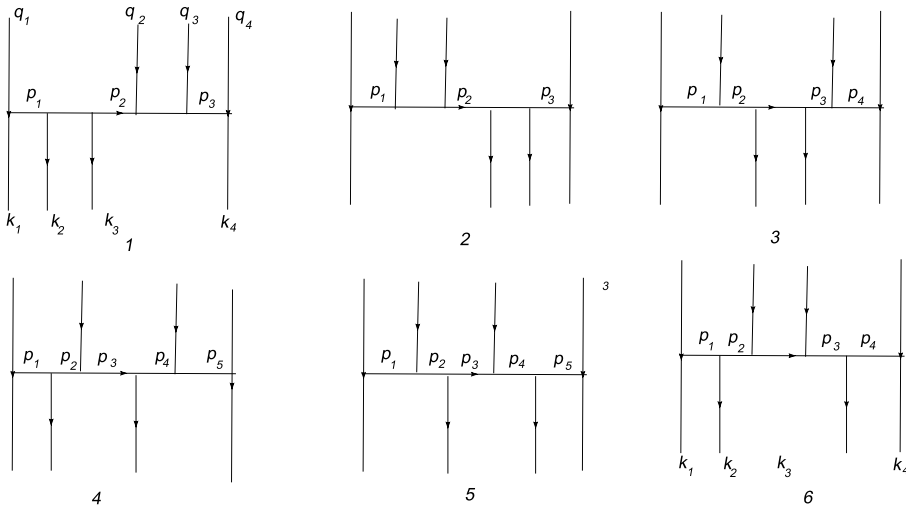


Figure 8. Kernel $K_{4 \rightarrow 4}$

and 5 are new. From parts one and two we find contributions $-g^2 d^{a_1 a_2 a_3 a_4} (F_2(q_1, q_{234}) + F_2(q_4, q_{123}))$.

From part 3 we find a term with the correct momentum structure $C_3 F_2(q_{12}, q_{34})$. but with the wrong color factor $C_3 = (d^{a_1 a_2 a_3 a_4} - d^{a_2 a_1 a_3 a_4})/2$ which does not correspond to (6) and violates the bootstrap.

No more terms depending on only one variable appear.

So we conclude that diagram Fig. 6,7 indeed gives two of the terms in (4). However the rest 5 terms are missing.

5 Conclusion

We have found that in successive splittings of the pomeron (fan diagrams) new diagrams with production of extra reggeons and higher splitting kernels $K_{2 \rightarrow n}$ with $n = 5$ and 6 provide the contributions which are needed to form the three-pomeron vertex at each splitting. This result agrees with conclusions in the framework of the dipole model, as expressed in the Balitski-Kovchegov equation.

In contrast, we have not been able to discover contributions needed to form two three-pomeron vertices in the transition $PP \rightarrow P \rightarrow PP$. A part of these contribution necessary to form one of the vertices was found from diagrams generated by kernels $K_{3 \rightarrow 4}$ and $K_{4 \rightarrow 4}$ but the rest is missing. So even the possibility to form one of the vertices Γ is questionable. If the necessary contributions are indeed absent then the vertex connecting the two initial and two final pomerons with the intermediate one reduces to just the simple kernel $K_{2 \rightarrow 2}$, that is to one half of the proper part of Γ .

References

- [1] V.S.Fadin, E.A.Kuraev, L.N.Lipatov, Phys. Lett. **B 60** (1975) 50; Ya.Ya. Balitsky, L.N.Lipatov, Sov. J. Nucl. Phys., **28** (1978) 822
- [2] J.Bartels, Z.Phys. **C 60** (1993) 471
- [3] J.Bartels and M.Wuesthoff, Z.Phys. **C 66** (1995) 157
- [4] A.H.Mueller, Nucl. Phys. **B 415** (1994) 373; **B 437** (1995) 107; A.H.Mueller and B.Patel, Nucl. Phys. **B 425** (1994) 471
- [5] M.A. Braun and G.P.Vacca, Eur. Phys. J. C **6** (1997) 147
- [6] I.Balitski, Nucl. Phys. **B 463** (1996) 99
- [7] Yu.V. Kovchegov, Phys.Rev **D 60** (1999) 034008
- [8] J.Bartels, M.Ryskin and G.P.Vacca, Eur. Phys. J. **C 27** (2003) 101
- [9] R. Peshanski. Phys. Lett. **B 409** (1997) 491
- [10] M.A.Braun, Eur. Phys. J. **C 63** (2009) 287
- [11] M.A.Braun and A.N. Tarasov, arXiv: 1304.3014
- [12] M.A.Braun, Eur. Phys. J. **48** (2006) 511
- [13] M.A.Braun, Eur.Phys.J. **c 16** (2000) 337
- [14] J.Bartels, L.N.Lipatov, G.P.Vacca, Nucl. Phys. **B 706** (2005) 391
- [15] J.Bartels, Nucl. Phys. **B 175** (1980) 365; J. Kwiecinski, M.Praszaloviicz, Phys. Lett. **B 94** (1980) 413
- [16] M.A.Braun, Eur. Phys. J. **C 6** (1999) 321
- [17] J.Bartels and C.Ewerz, JHEP **9909** (1999) 026
- [18] J.Bartels, Nucl. Phys. **B 175** (1980) 365